

Spatial and temporal characterization of climate at regional scale using homogeneous monthly precipitation and air temperature data: an application in Calabria (southern Italy)

T. Caloiero, G. Buttafuoco, R. Coscarelli and E. Ferrari

ABSTRACT

In the present study, an approach for a climate characterization based on a statistical analysis of monthly precipitation and temperature data is presented. First, the original database (1916–2010) was homogenized and a geostatistical analysis was carried out to characterize the monthly mean distribution of the two variables in the study area. Then, temporal change of precipitation and temperature were evaluated through the Mann–Kendall test. Finally, to better assess the climate patterns in Calabria, a climatic characterization was carried out by means of the Péguy climograph. Results have shown a decreasing trend for autumn–winter rainfall and an increasing trend in summer. With respect to the average temperature, the analyses revealed a positive trend in late spring and summer, mainly due to the increase in the minimum values, and a negative trend in the autumn–winter period, mainly due to a decrease in the maximum values. The analysis of the Péguy climographs allowed the dataset to be divided into three groups, depending on the different elevation of the gauges. Moreover, different temporal behaviours were detected by analysing the climographs in three sub-periods.

Key words | air temperature, Calabria, geostatistics, precipitation, trend

T. Caloiero
G. Buttafuoco
CNR-ISAFOM,
Rende (CS),
Italy

R. Coscarelli
CNR-IRPI,
Rende (CS),
Italy

E. Ferrari (corresponding author)
DIMES,
University of Calabria,
Rende (CS),
Italy
E-mail: ennio.ferrari@unical.it

INTRODUCTION

In recent years, with growing concerns about climate change impacts, precipitation and air temperature have become the most investigated meteorological variables because of their influence on all natural systems and human activities, including agriculture, water quantity and quality, ecosystems, and human health (IPCC 2013). In particular, decreasing water quality and changes in its spatial and temporal distribution have become one of the most crucial issues for their environmental and socio-economic implications (Incerti *et al.* 2007; Helldén & Tottrup 2008; Zhou & Wang 2011).

As regards the temporal distribution of rainfall, some decreases in annual precipitation in the Mediterranean area have been detected (Xoplaki *et al.* 2006; Feidas *et al.* 2007; del Rio *et al.* 2011). In Italy, the existence of a

decreasing trend in annual precipitation has been identified by many regional studies (Palmieri *et al.* 1991; Brunetti *et al.* 2006b, 2012; Pavan *et al.* 2008; Caloiero *et al.* 2011a, b), while other regional studies did not detect any significant trend at all (Von Hardenberg *et al.* 2008; Fatichi & Caporali 2009). On seasonal and monthly time scales, in northern and central Italy, Brunetti *et al.* (2006a) found a decreasing rainfall trend more evident in spring, while Ventura *et al.* (2002) and Vergni & Todisco (2011) showed that decreases occur only during autumn and winter. As regards winter precipitation, Toreti *et al.* (2009) detected a positive trend in central Italy and a negative trend in northern Italy. In southern Italy, and particularly in the Calabria region, different studies (Buttafuoco *et al.* 2011; Caloiero *et al.* 2011a, b; Brunetti *et al.* 2012; Capra *et al.* 2013; Ferrari *et al.* 2013)

highlighted a decreasing trend in winter and autumn rainfall, and an increasing trend in spring and summer.

As to what concerns temperature, the increase in mean values over the last century has been largely demonstrated in many studies focused on different regions of the world on a large spatial scale (Klein Tank & Können 2003; Vose *et al.* 2005; Klok & Tank 2009) or at national and local spatial scale (Brunetti *et al.* 2004, 2006a; Toreti & Desiato 2008; del Rio *et al.* 2012). The magnitude of trends differs according to the area and the period studied, especially when comparing the rate in increase of maximum and minimum temperatures. In particular, Klok & Tank (2009), for the whole of Europe, Sánchez *et al.* (2004), for the Mediterranean, and Toreti & Desiato (2008), for Italy, have highlighted the fact that the maximum temperatures have increased at a higher rate than the minimum ones. Donat & Alexander (2012) used a global dataset of daily temperatures to show that both day-time (daily maximum) and night-time (daily minimum) temperatures have become higher over the past 60 years: changes were greater for minimum than for maximum values.

Precipitation and temperature vary more or less continuously in a geographical space and could be regarded as regionalized variables (Matheron 1971). Geostatistics provides a valuable tool for the study of the spatial correlation in data by creating mathematical models, commonly expressed by semivariograms. The interpolation technique of the variable, known as kriging, provides an unbiased linear estimate of a regionalized variable in an unsampled location (Chilès & Delfiner 2012). Examples of geostatistical studies on precipitation and temperature can be found in Hudson & Wackernagel (1994), Diodato & Ceccarelli (2005), Grimes & Pardo-Iguzquiza (2010), Buttafuoco *et al.* (2011), Aznar *et al.* (2013), Bajat *et al.* (2013) and Diodato *et al.* (2013).

This investigation presents an analysis of the spatial and temporal behaviour of monthly precipitation and temperature in the Calabria region (southern Italy). In the 'Methodology' section, the procedures used for the analysis are presented, with particular concern as regards the geostatistical techniques. In the 'Study area and data' section, the geographical and climatic features of the Calabria region and the homogenized databases of rainfall and temperature are described. In the 'Results and discussion' section, firstly the spatial distributions of the monthly mean values of both

precipitation and temperature in the study area for the whole observation period (1916–2010) have been described. Then, in the same section, in order to better investigate the link between the two variables, the Péguy climograph (Péguy 1961) was drawn for different ranges of the station elevations. Moreover, the tendencies of rainfall and temperature at monthly and seasonal scales were investigated separately through the application of the non-parametric Mann–Kendall test. Finally, in order to test the temporal variability of the climatic features on the study area, the Péguy climographs were built with reference to three sub-periods (1921–1950, 1951–1980, 1981–2010).

METHODOLOGY

Meteorological time series cannot be used for climate research without clear knowledge of data homogeneity. Actually, the real climate signal can be hidden behind non-climatic noise caused by changes in instruments and algorithms for statistical calculation, station relocation, changes in observation procedures, and so on (Brunetti *et al.* 2012). In fact, homogeneity testing and adjustment of climatic time series for non-climatic variations are a fundamental part of any climate change analysis (Alexandersson 1986; Karl & Williams 1987; Peterson & Easterling 1994; Jones 1995). In this work, a homogenization approach similar to that discussed in Brunetti *et al.* (2012) for precipitation was adapted to the temperature. Due to the low number of temperature stations available for this analysis, as described in the following section, each series was tested against other ones, in sub-groups of five series, by means of a multiple application of the Craddock test (Craddock 1979). When an inhomogeneity (break) was identified, the series used to estimate the adjustments were chosen among the neighbouring series that were homogeneous in a sufficiently long sub-period centred on the break year, and which correlate well with the candidate one. The adjustments from each reference series were calculated on a monthly basis.

Then, the mean precipitation and temperature data for each month of the year were modelled as an intrinsic stationary process using a geostatistical approach, where each datum $z(\mathbf{x}_\alpha)$ measured at \mathbf{x}_α (\mathbf{x} is the location coordinates vector and α the sampling points = 1, ..., N) is

interpreted as a particular realization of a random variable $Z(\mathbf{x}_\alpha)$ (Goovaerts 1997; Wackernagel 2003; Webster & Oliver 2007; Chilès & Delfiner 2012). The set of random variables $Z(\mathbf{x}_1), Z(\mathbf{x}_2), \dots$, constitutes a random function. The set of actual values of Z that comprises the realization of the random function is known as a regionalized variable $z(\mathbf{x}_\alpha)$. Interested readers should refer to textbooks such as Goovaerts (1997), Chilès & Delfiner (2012), Wackernagel (2003), Webster & Oliver (2007), among others, for a detailed presentation of the theory of the regionalized variables. An objective of geostatistics is to quantify and exploit spatial pattern of regionalized variables. The quantitative measure of spatial correlation of the regionalized variable $z(\mathbf{x}_\alpha)$ is the experimental variogram $\gamma(\mathbf{h})$, which is a function of the distance vector (\mathbf{h}) of data pairs values $[z(\mathbf{x}_\alpha), z(\mathbf{x}_\alpha + \mathbf{h})]$. A theoretical function, called variogram model, is fitted to the experimental data to analytically estimate the variogram for any distance \mathbf{h} . The variogram model generally requires two parameters: range and sill. The range is the distance over which pairs of regionalized variable values are spatially correlated, while the sill is the variogram value corresponding to the range.

The optimal fitting is chosen on the basis of a cross-validation. The goodness of fit is evaluated by the mean error (ME) and the mean squared deviation ratio (MSDR). The ME proves the unbiasedness of estimate if its value is close to 0. The MSDR is the ratio between the squared error and the kriging variance (Webster & Oliver 2007), and if the model for the variogram is accurate, its value should be 1. The fitted variograms for both the measured mean monthly precipitation and temperature data were used to estimate their values at ungauged locations using a variant of kriging. Precipitation was predicted using Ordinary Kriging (OK) (Webster & Oliver 2007), whereas, since monthly mean temperature data are available only at few locations, and temperature is generally well correlated with elevation, a variant of kriging known as Kriging with External Drift (KED) was adopted using elevation as secondary information (Hudson & Wackernagel 1994).

In the scope of KED, the variable of interest $Z(\mathbf{x})$ is represented through deterministic and stochastic components:

$$Z(\mathbf{x}_\alpha) = m(\mathbf{x}) + \varepsilon(\mathbf{x}) \quad \text{and} \quad E[Z(\mathbf{x})] = m(\mathbf{x}) \quad (1)$$

where $\varepsilon(\mathbf{x})$ is the stochastic component with zero mean and variogram $\gamma_\varepsilon(\mathbf{h})$, and $m(\mathbf{x})$ is the drift, which is usually modelled as a linear function of a smoothly varying secondary (external) variable $y(\mathbf{x})$ (in this case, elevation):

$$m(\mathbf{x}) = a_0(\mathbf{x}) + a_1(\mathbf{x})y(\mathbf{x}) \quad (2)$$

The two coefficients $a_0(\mathbf{x})$ and $a_1(\mathbf{x})$ are deemed constant within the search neighbourhood and are implicitly estimated through the kriging system (Goovaerts 1997).

In this study, the values of precipitation and temperature were estimated at the nodes of a 250×250 m interpolation grid, and all geostatistical analyses were performed using the software Isatis®, release 2013.3 (<http://geovariances.com>).

Moreover, monthly data were used to outline Péguy climographs (Péguy 1961), where mean values of both mean monthly temperatures ($^{\circ}\text{C}$) and precipitation (mm) are reported on the x -axis and on the y -axis, respectively. A triangular reference polygon, having coordinates (0°C ; 0 mm), (23°C ; 45 mm), and (16°C ; 200 mm), divides the Cartesian space in four climatic regions, correspondent to the dominant character of the month: (a) temperate, months falling within the triangle; (b) arid, months below the alignment (0°C ; 0 mm), (23°C ; 45 mm); (c) tropical, months on the right side of the alignment (23°C ; 45 mm), (16°C ; 200 mm) and (d) cold, months on the left side of the alignment (0°C ; 0 mm), (16°C ; 200 mm).

Finally, the precipitation and temperature datasets were also analysed for trend, with significance assessed through the Mann–Kendall non-parametric test, widely used since normality or linearity are not required (Mann 1945; Kendall 1962).

STUDY AREA AND DATA

The Calabria region occupies the southern part of the Italian peninsula (Figure 1). It has an area of $15,080 \text{ km}^2$ and a coastline of 738 km on the Ionian and Tyrrhenian seas. To the north, it borders the Basilicata region for 80 km. The Calabria region has an oblong shape with a length of 248 km and a width ranging between 31 and 111 km. Although Calabria does not have many high summits, it is one of the most mountainous regions in Italy (Figure 1): 42% of the land is mountainous (elevation greater

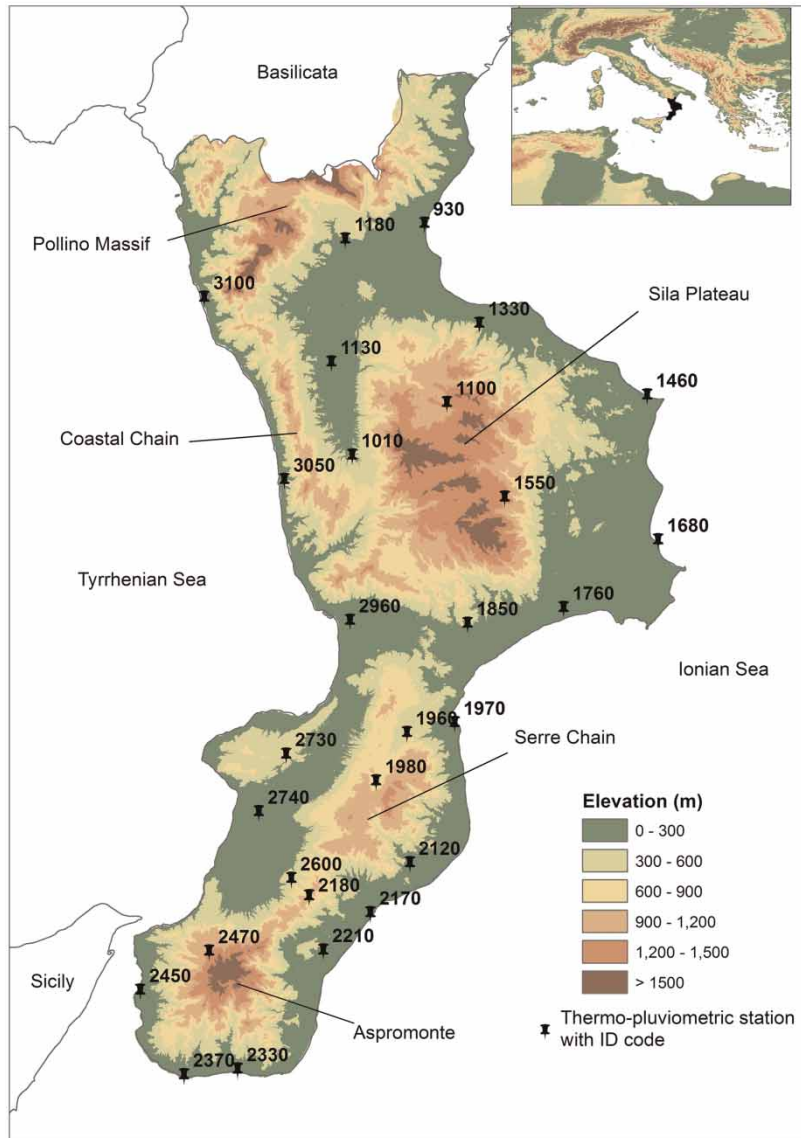


Figure 1 | Location of the selected stations with code (ID) on a DEM of Calabria.

than 500 m above sea level (a.s.l.), 49% hilly (elevation between 50 and 500 m a.s.l.) and only the 9% is flat (elevation lower than 50 m a.s.l.). The maximum elevation is 2,267 m a.s.l., while the average elevation is 597 m a.s.l.

Because of its geographic position and mountainous nature, Calabria has a high climatic variability (Coscarelli & Caloiero 2012) with a typically dry summer subtropical climate, also known as the Mediterranean climate. The coastal zones are characterized by mild winters and hot summers with little precipitation. In particular, the Ionian side,

which is influenced by currents coming from Africa, has high temperatures with short and heavy precipitation, while the Tyrrhenian side is influenced by western air currents and presents milder temperatures and considerable orographic precipitation. In the inland zones there are colder winters (with snow) and fresher summers (with some precipitation) than those marking the coastal zones (Caloiero et al. 2011a).

Daily precipitation and air temperature data, for the Calabria region, have been collected since 1916 by the

former Italian Hydrographic Service, now Centro Funzionale Multirischi Arpacal. The data used in this study are a set of monthly precipitation and air temperature series registered in Calabria for the period 1916–2010. In particular, the precipitation database was extracted from the homogeneous one presented in Brunetti *et al.* (2012), consisting of 129 rainfall series, updated to 2010. The whole database was used only for the spatial analysis of rainfall. Further analyses were conducted using only the rainfall data given by gauges in which both rainfall and temperature data were present. As regards temperature, the homogenization procedure was applied to both maximum and minimum series having more than 50 years of observation. As a result, 16 out of 34 monthly temperature series were homogeneous, while six series were discarded due to their very low quality. A total of 12 series were homogenized, by correcting 25 and 27 breaks for the maximum and minimum temperature, respectively. Finally, the dataset used for the analysis included 28 stations, with a density of about one gauge per 530 km² (Figure 1).

RESULTS AND DISCUSSION

Basic statistics of regional precipitation and temperature data are presented in Tables 1 and 2, respectively. With reference to the mean values, December (163.5 mm) is the rainiest month of the year, while the driest month is July (17.8 mm). January is the coldest month (8.2 °C), while

August is the warmest one (24.5 °C). The skewness of the precipitation data ranges from 0.06 to 0.58 (Table 1) and no transformation was considered to remove asymmetry. On the contrary, the skewness of the temperature data ranges from –0.80 to –1.3 (Table 2) and for subsequent analyses they were transformed into a Gaussian variable, and standardized to zero mean and unit variance using the Gaussian anamorphosis (Wackernagel 2003) by an expansion of Hermite polynomials (Rivoirard 1994) restricted to the first 30 terms. The transformed data were used in the interpolation process and then the kriging results were back-transformed to the raw distribution.

To check the behaviour of elevation in terms of stationarity and anisotropy, monthly variogram maps were calculated for each variable. Variogram maps (not shown) for monthly mean precipitations and temperatures clearly showed the same behaviours of the experimental variograms in different directions so that an isotropic model was fitted to them. The parameters of the fitted model are reported in Tables 3 and 4 respectively. The fitted variogram models for mean monthly precipitations were nested and included mainly a nugget effect, a short-range spherical model (Webster & Oliver 2007) and a long-range spherical model (Table 3). The nugget effect implies a discontinuity in the random function $Z(\mathbf{x})$ and is a positive intercept of the variogram. It arises from errors of measurement and spatial variation within the shortest sampling interval (Webster & Oliver 2007).

Table 1 | Regional statistics for mean monthly precipitation expressed in mm (129 rain gauges)

Variable	Minimum	Maximum	Mean	Stand Dev	Skewness	Lower quartile	Median	Upper quartile
January	57.6	282.9	149.5	49.8	0.54	111.3	142.9	181.8
February	49.5	218.8	115.8	43.1	0.54	85.5	106.8	145.0
March	42.2	205.0	103.9	34.4	0.58	78.4	95.3	124.0
April	26.7	157.8	73.1	27.5	0.50	53.4	70.5	93.1
May	15.9	106.8	50.3	19.5	0.51	34.6	49.2	61.8
June	4.9	51.7	25.3	10.6	0.23	17.0	25.2	32.2
July	2.4	38.6	17.8	7.3	0.06	12.9	17.7	22.6
August	7.1	50.3	25.1	8.2	0.22	19.0	25.7	30.3
September	26.0	114.7	62.4	15.0	0.54	52.2	61.2	70.5
October	43.3	204.7	119.4	29.1	0.29	101.3	117.2	138.7
November	49.8	252.9	149.2	43.0	0.40	118.1	140.9	178.3
December	54.0	297.5	163.5	52.0	0.53	125.6	154.4	193.9

Table 2 | Regional statistics for mean monthly temperature expressed in °C (28 temperature gauges)

Variable	Minimum	Maximum	Mean	Stand Dev	Skewness	Lower quartile	Median	Upper quartile
January	0.9	11.6	8.2	2.9	-0.97	6.2	8.9	10.3
February	1.4	12.3	8.5	3.0	-0.87	5.8	9.3	10.7
March	3.3	13.2	10.3	2.7	-1.14	8.8	11.1	12.3
April	6.4	15.6	12.9	2.7	-1.13	11.4	13.9	14.9
May	10.6	19.7	17.2	2.5	-1.30	15.7	18.1	19.1
June	14.8	24.1	21.3	2.7	-1.14	19.7	22.3	23.3
July	17.5	27.2	24.2	2.9	-1.16	22.4	24.9	26.5
August	17.5	27.5	24.5	2.9	-1.24	22.8	25.4	26.6
September	14.5	24.4	21.2	3.0	-1.00	19.2	22.2	23.6
October	10.2	20.6	17.2	2.8	-1.05	15.3	18.1	19.4
November	6.4	16.9	13.0	2.9	-0.80	10.7	13.9	15.3
December	2.3	14.0	9.5	2.9	-0.84	7.3	10.3	11.7

Table 3 | Variogram model parameters for monthly mean precipitation

Variable	Model	Sill (mm ²)	Range (m)	Variable	Model	Sill (mm ²)	Range (m)
January	Nugget effect	558.66		August	Nugget effect	2.33	
	Spherical	1,004.63	29,583.6		Spherical	33.66	31,262.9
	Spherical	903.67	40,698.9		Spherical	21.18	40,516.0
February	Nugget effect	294.16		September	Nugget effect	40.87	
	Spherical	1,028.26	46,505.8		Spherical	24.89	29,593.3
	Exponential	574.61	135,243.8		Spherical	141.66	51,822.0
March	Nugget effect	153.33		October	Nugget effect	112.74	
	Spherical	996.24	30,565.3		Spherical	445.53	31,243.7
April	Nugget effect	131.50		November	Nugget effect	271.45	
	Spherical	597.56	46,946.4		Spherical	639.59	28,103.3
May	Nugget effect	36.21		Spherical	910.84	44,955.9	
	Spherical	346.03	53,577.9	December	Nugget effect	488.07	
June	Nugget effect	4.40			Spherical	766.12	27,180.7
July	Spherical	100.56	41,846.4		Spherical	1,427.75	43,998.3
	Spherical	7.34	25,403.8				
	Spherical	39.18	41,499.6				

The spherical model (Webster & Oliver 2007) is

$$\gamma(h) = \begin{cases} c \left[\frac{3h}{2a} - \frac{1}{2} \left(\frac{h}{a} \right)^3 \right] & \text{for } 0 < h \leq a \\ c & \text{for } h > a \end{cases} \quad (3)$$

where a is the range and c the sill.

Only for February, the fitted variogram included a nugget effect, a short-range spherical model and a long-range exponential model (Table 3). The exponential model (Webster & Oliver 2007) is

$$\gamma(h) = c \left[1 - \exp\left(-\frac{h}{r}\right) \right] \quad (4)$$

Table 4 | Variogram model parameters for monthly mean temperature

Variable	Model	Sill (-)	Range (m)	Variable	Model	Sill (-)	Range (m)
January	Nugget effect	0.2532		July	Nugget effect	0.4033	
	Spherical	0.6625	14,407.4		Spherical	0.7385	25,463.2
February	Nugget effect	0.1787		August	Nugget effect	0.2929	
	Spherical	0.7593	20,356.1		Spherical	0.8252	24,885.1
March	Nugget effect	0.1764		September	Nugget effect	0.2929	
	Spherical	0.8446	29,205.9		Spherical	0.2929	24,885.1
April	Nugget effect	0.0300		October	Nugget effect	0.1045	
	Spherical	0.9783	28,546.4		Spherical	0.8575	23,150.7
May	Nugget effect	0.4727		November	Nugget effect	0.1616	
	Spherical	0.6567	25,270.5		Spherical	0.8061	28,161
June	Nugget effect	0.3235		December	Nugget effect	0.2473	
	Spherical	0.8223	22,572.6		Spherical	0.7000	26,619.4

where r is a distance parameter that defines the spatial extent of the model. The exponential model approaches its sill asymptotically and so has no finite range. For practical purposes, a practical range has been taken as the distance at which the variogram value equals 95% of the sill variance (approximately $3r$).

The nested variogram with two models at shorter and longer scales describes two scales of variation, probably due to different processes.

The fitted variogram models for the Gaussian values of mean monthly temperature (Table 4) were nested and included a nugget effect and a spherical model. The goodness of fitting of all variogram models was verified by cross validation. The results were quite satisfactory because the statistics used, i.e. mean of the estimation error and variance of the MSDR, were quite close to 0 and 1, respectively.

The values of the mean monthly precipitation were predicted at the nodes of the interpolation grid using OK and mapped (Figure 2).

The values of the Gaussian mean monthly temperature were predicted at the nodes of the interpolation grid using KED. The predicted values of temperature were back transformed to the raw data through the mathematical model calculated in the Gaussian anamorphosis and mapped (Figure 3).

Monthly climatic characteristics were obtained through the Péguy climographs of the 28 stations in which both temperature and precipitation data were available (Figure 4). As a

result, three groups of stations were identified with a different behaviour of the climograph. In the first one (Figure 4(a)), the thermo-pluviometric stations are characterized by arid climate for 3–5 months, while the remaining months have a temperate climate; these stations are all located near the coast with an altitude lower than about 80 m a.s.l. A second group of stations presents similar behaviour but with 1–3 months characterized by cold climate; in this case the stations elevation ranges from 80 to about 400 m a.s.l. In the third one, cold conditions are clearly shown, with 5–6 months which present cold climate and fewer months (1–2) with arid climate. The stations of the latter group are all located at the highest altitudes (>400 m a.s.l.).

As expected, the climate conditions are quite different between high and low altitude stations, mainly during cold months. This aspect plays an important role on evapotranspiration and infiltration processes. In fact, high mean temperature values, coupled with a low amount of rainfall, are the main reasons that could trigger desertification processes in the topographically low areas of the region. However, other morphological features, besides altitude (e.g. continentality and exposition), could affect climate conditions.

The results of the application of the trend analysis (statistical significance: 95%) to the monthly and seasonal precipitation series are shown in Figure 5 and Table 5. With regards to the seasonal precipitation, a general negative trend was detected for the 1916–2010 period, in particular for the

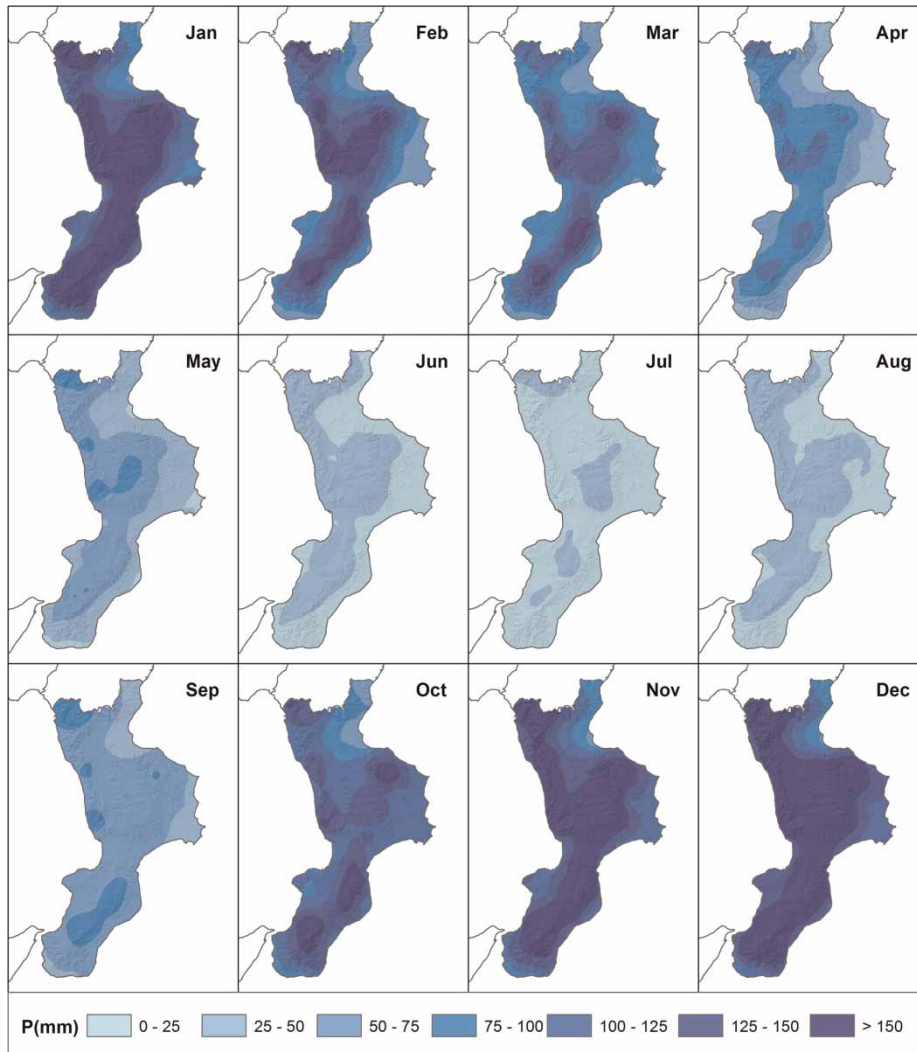


Figure 2 | Maps of mean monthly precipitation obtained using OK (129 rain gauges).

autumn and winter period (Figure 5(a) and Table 5). In fact, 50 and 25% of the rain gauges show a negative trend, with a maximum decreasing rate of -57.8 mm/10 years and -32.9 mm/10 years in winter and autumn respectively. On a monthly scale, a negative trend was detected in January (35.7% of the rain gauges) and November (53.6%), with maximum decreases of -24.8 mm/10 years and -23.6 mm/10 years respectively. A negative trend was also found in September (28.6% of the rain gauges), with a maximum rate of -25.8 mm/10 years. Conversely, summer precipitation shows positive trends, in particular in July (21.4% of the data series) and August (17.9%), with a maximum positive trend of $+1.7$ mm/10 years and $+2.3$ mm/10 years respectively.

The results of the trend analysis performed on the 28 temperature series are shown in Figure 5 and Tables 6–8. In particular, the average temperature (Figure 5(b) and Table 6) shows a positive trend from May to August, with a percentage of stations between 25 and 33.3% and a maximum trend ($^{\circ}\text{C}/10$ years) ranging from $+0.23$ to $+0.32$. A negative trend was detected in September and November, respectively for 46 and 35% of the temperature series with a maximum trend of -0.36 $^{\circ}\text{C}/10$ years and -0.32 $^{\circ}\text{C}/10$ years. On a seasonal scale results show a positive trend in spring (18% of the stations and $+0.18$ $^{\circ}\text{C}/10$ years) and summer (29% and $+0.34$ $^{\circ}\text{C}/10$ years), while in autumn a negative trend for 39% of the series was detected with a maximum reduction of -0.30 $^{\circ}\text{C}/10$ years.

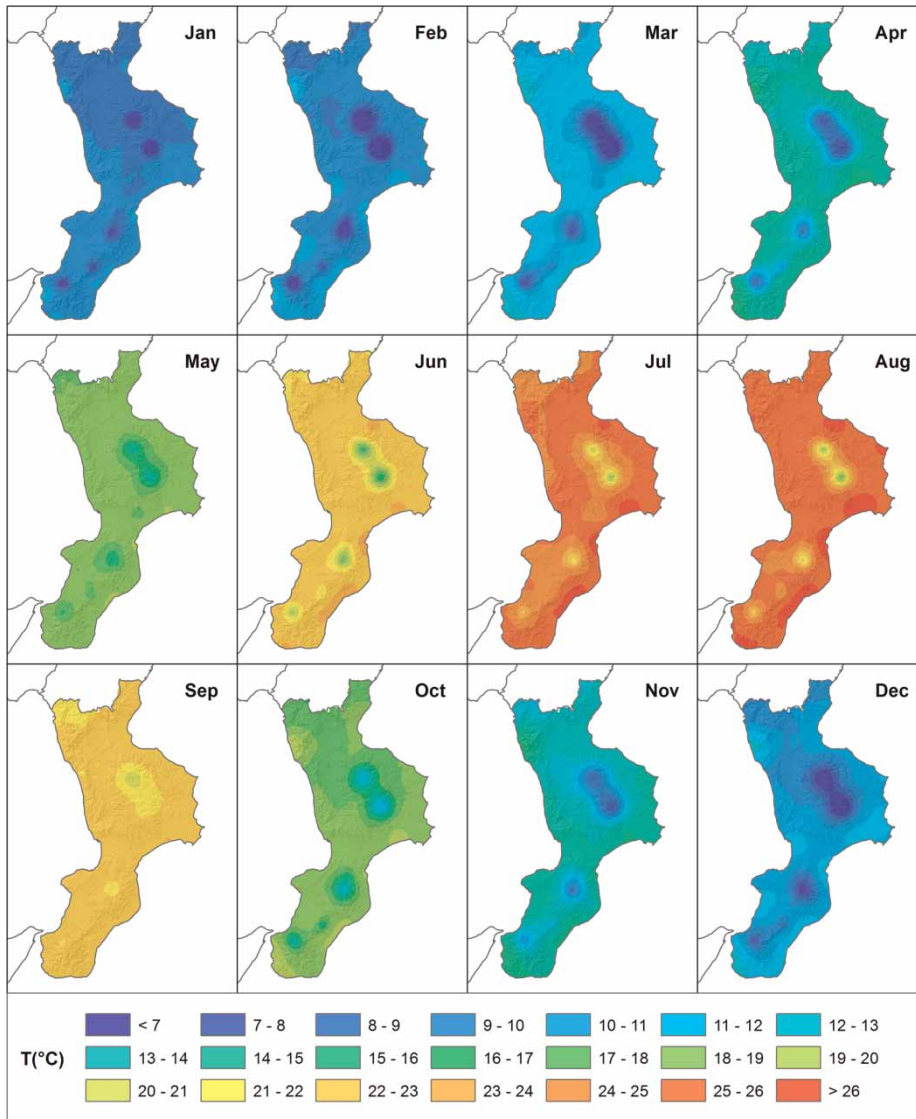


Figure 3 | Maps of mean monthly temperature obtained using KED (28 temperature gauges).

The maximum temperatures (Figure 5(c) and Table 7) show a downward trend both on monthly and seasonal scales. Only in the month of May, there is the prevalence of a positive trend (21% of the stations and a maximum positive trend of $+0.33\text{ }^{\circ}\text{C}/10\text{ years}$), while for the months of January and June there is no clear tendency. For the remaining months there is a prevalence of negative trend, more evident in September (74% of the stations and a maximum decreasing rate of $-0.57\text{ }^{\circ}\text{C}/10\text{ years}$), April (39% and $-0.48\text{ }^{\circ}\text{C}/10\text{ years}$), November (36% and $-0.48\text{ }^{\circ}\text{C}/10\text{ years}$), August (30% and $-0.69\text{ }^{\circ}\text{C}/10\text{ years}$)

and July (29% and $-0.84\text{ }^{\circ}\text{C}/10\text{ years}$). At seasonal scale a clear negative tendency in maximum temperatures emerged, ranging from 21% (summer) to 57% (autumn) of the stations.

As regards the minimum temperatures (Figure 5(d) and Table 8), a positive trend for almost all the months was observed, with percentages ranging from 18% (March) to 50% (May) of the stations and maximum rate of $+0.49\text{ }^{\circ}\text{C}/10\text{ years}$ (June). Only the months of November and February show a prevalence of negative trend (30 and 25% of the stations, and maximum negative rates of $-0.29\text{ }^{\circ}\text{C}/10\text{ years}$

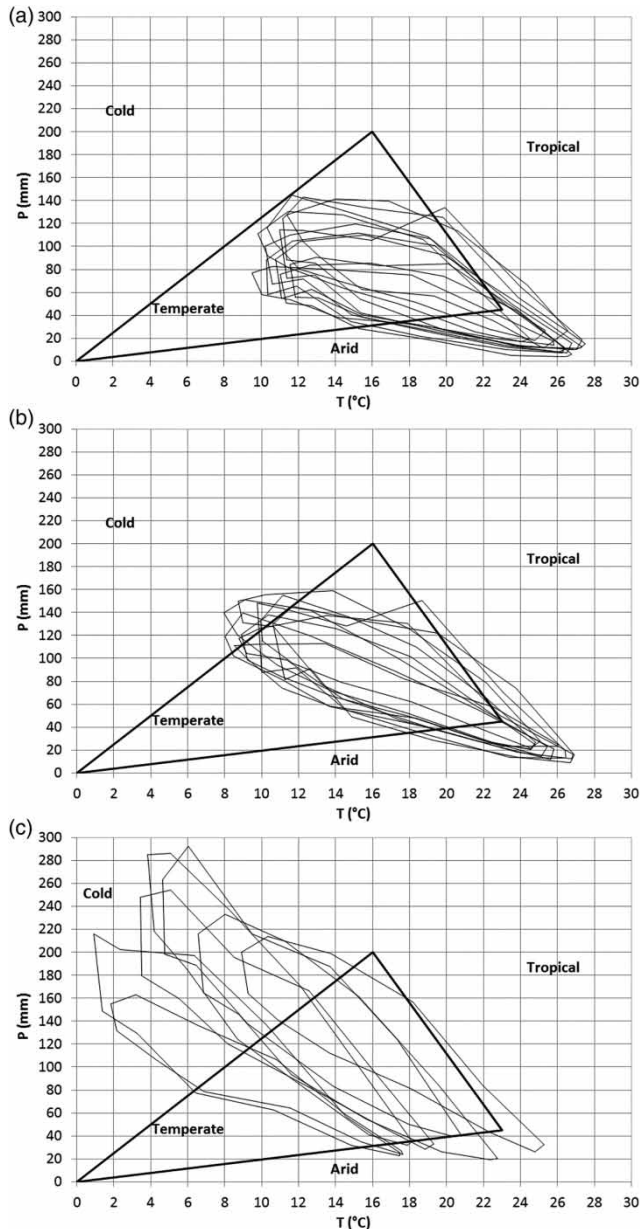


Figure 4 | Peguy climatographs for the set of 28 thermo-pluviometric series: (a) gauges with elevation lower than 80 m a.s.l.; (b) gauges with elevation from 80 to 400 m a.s.l.; (c) gauges with elevation higher than 400 m a.s.l.

and $-0.40^{\circ}\text{C}/10$ years, respectively). At seasonal scale a positive trend was shown in spring and summer (39% of stations in both cases).

These results confirm the analyses conducted at the end of the 20th century which have remarked that minimum temperatures are increasing more than the maximum temperatures at planetary scale (Easterling et al. 1997), although

some different results have been presented in the literature for some European regions (e.g. Toreti & Desiato 2008).

Finally, due to the variations of precipitation and temperature in the time series detected, in order to assess possible local temporal change in climate conditions, the Péguy climatographs were also evaluated for each gauge and for three different time periods (1921–1950, 1951–1980 and 1981–2010). The results show different behaviours of the climatographs in the three sub-periods, due mainly to a widespread decrease in monthly winter rainfall and, partially, to variations in summer temperature. The influences of rainfall and temperature on the different temporal shapes of the climatographs reflect the tendencies evidenced by the two variables in the trend analyses: a maximum monthly rainfall variation in winter equal to -24.8 mm/10 years and a maximum monthly average temperature variation in summer equal to $+0.32^{\circ}\text{C}/10$ years.

The most evident results of the sub-periods analysis is the tendency of the climatographs to move towards temperate conditions. In particular, for the gauges located near the coasts (e.g. Figures 6(a) and (b)) winter months characterized by cold conditions during the period 1921–1950 present temperate conditions in the last sub-period. The gauges located at higher elevations, but below 400 m a.s.l., show a progressive reduction in the number of cold winter months, with a tendency to temperate conditions (e.g. Figures 6(c) and (d)). Finally, for the gauges located above 400 m a.s.l. (e.g. Figures 6(e) and (f)) no change in climatic conditions was observed, although a marked variation in the climatograph's shape clearly exists due to the severe reduction in winter monthly rainfalls. As a general result, for almost all the gauges the sub-period 1981–2010 presents a different climatograph's shape with respect to those of the other sub-periods.

CONCLUSIONS

Due to its geographic position and mountainous nature, Calabria is a region with highly varying climatic features depending on various factors (e.g. elevation, exposition, distance from the sea). For this reason a satisfying spatial and temporal characterization of climate required both good quality data for the temporal analysis and statistical tools

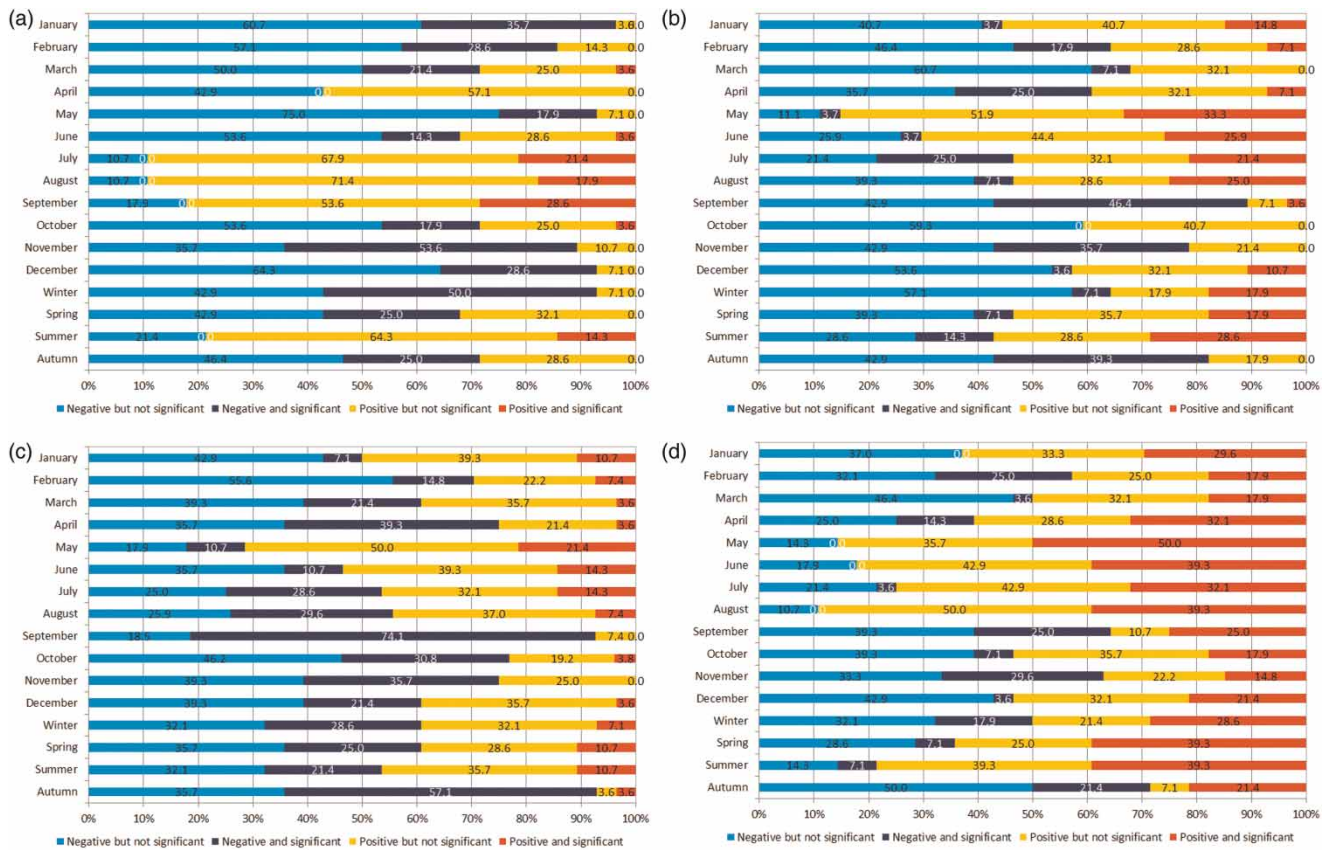


Figure 5 | Rainfall and temperature trend results for the 28 termo-pluviometric gauges, expressed as % of the whole data set: (a) rainfall; (b) minimum temperature; (c) mean temperature; (d) maximum temperature.

to take into account the spatial autocorrelation of data. In particular, the monthly database available in Calabria for rainfall and temperature variables underwent thorough qualitative checks. In fact, homogeneity testing and subsequent adjustment of the climatic time series from non-climatic variations provided a good quality database of 28 monthly time series.

For the spatial investigation, a variographic analysis was performed and two different interpolation techniques were adopted: an OK for rainfall and a KED with elevation as external drift for temperature. This latter method was chosen because of a smaller number of temperature gauges, whose data are yet strictly correlated with the elevation.

Monthly climatic characteristics were studied through the Péguy climatographs of the 28 stations in which both temperature and precipitation data are available. As a result, three groups of stations were identified: the first is characterized by

arid and temperate climate, with stations located near the coast. The second group of stations presents a similar behaviour but also with cold climate and elevation lower than 400 m a.s.l. The third, including stations located at the highest altitudes, is mostly characterized by cold conditions.

The results of the trend analysis for monthly and seasonal precipitation series showed a general negative trend for the 1916–2010 period, in particular for the autumn and winter periods. As concerns the average temperature values, trend analysis showed a positive trend in the late spring and summer period, and a negative trend in autumn. The maximum temperature showed a downward trend both on monthly and seasonal scales, while a positive trend for almost all the months was observed for the minimum temperature.

Finally, the analysis of the Péguy climatographs for three different time periods showed different behaviours, mainly due to a widespread decrease in monthly winter rainfall and, partially, to variations in summer temperature.

Table 5 | Results of the trend analysis (mm/10yrs) for the monthly and seasonal precipitation (significant values are marked in bold)

ID	January	February	March	April	May	June	July	August	September	October	November	December	Winter	Spring	Summer	Autumn
930	-6.6	-2.4	-0.4	-0.5	-2.6	0.3	1.7	-0.1	1.4	-3.7	-3.4	-5.5	-15.2	-3.1	2.2	-3.8
1010	-1.1	-3.6	0.1	-1.7	-1.6	0.7	-0.1	0.4	1.5	-3.1	-1.2	-4.8	-8.7	-2.7	1.1	-2.3
1100	-6.3	-7.9	-2.2	1.2	-6.1	0.0	-0.3	1.9	0.4	-3.6	-9.2	-4.7	-21.0	-6.2	2.1	-10.0
1130	-1.2	-2.3	-0.1	2.0	-0.6	1.2	0.9	1.2	3.5	-0.5	-1.6	-1.9	-6.6	2.0	3.4	2.0
1180	-4.0	-2.3	0.3	0.8	-1.6	0.5	0.8	0.3	1.5	0.1	-3.6	-4.7	-11.3	-0.4	1.8	-1.6
1330	-2.3	-1.4	-1.5	-2.0	-3.5	-1.3	2.2	1.1	4.7	2.2	-8.0	0.5	0.4	-5.8	1.8	-1.5
1460	-4.6	-2.5	0.3	0.9	0.2	-1.5	0.7	1.8	3.6	-0.3	-5.5	-7.3	-17.6	1.1	0.9	-3.1
1550	-15.4	-11.0	-4.7	-1.2	-4.0	-3.3	0.1	0.8	-1.6	-0.8	-23.6	-15.5	-41.2	-10.2	-2.5	-22.9
1680	-1.2	-2.4	0.9	1.5	0.4	0.0	1.7	0.3	3.3	-1.2	-6.8	-1.3	-5.7	4.1	2.0	-4.8
1760	-3.2	-7.3	-1.4	0.5	-1.5	-0.8	1.7	0.1	3.4	-1.9	-14.9	-4.1	-16.1	-2.1	1.0	-11.8
1850	-6.7	-7.7	-4.6	-1.8	-1.4	-1.4	1.4	1.3	0.6	-6.7	-8.1	-1.8	-18.8	-7.1	1.4	-14.3
1960	-4.6	-11.8	-6.8	-3.1	-2.3	-1.6	1.3	0.8	7.5	-9.5	-16.9	-3.5	-23.8	-11.0	0.5	-20.8
1970	-8.6	-8.2	-6.2	-2.4	-1.9	-1.3	0.6	-0.8	3.0	-10.6	-19.0	-13.1	-32.1	-10.8	-1.3	-25.1
1980	-8.4	-10.7	-9.3	2.1	-2.7	-1.6	2.1	3.0	7.2	-3.2	-13.6	-3.3	-23.0	-8.5	2.7	-7.1
2120	-6.1	-2.6	-5.4	1.3	-2.9	-1.8	0.7	2.2	11.7	-30.7	-15.2	3.4	-6.9	-6.9	0.5	-32.9
2170	-3.9	-2.5	-1.6	1.1	0.2	-1.1	0.4	2.2	3.9	-8.2	-4.4	-3.3	-10.1	-0.5	0.6	-8.8
2180	-0.5	-6.0	-5.7	4.1	1.0	4.3	-2.5	3.9	25.8	-12.1	17.1	-12.7	-26.5	0.0	6.7	30.8
2210	-1.5	-2.0	-0.1	0.4	-1.1	0.3	1.3	0.2	9.2	1.0	-12.8	-4.7	-6.1	-0.1	1.7	-2.1
2330	-2.5	-3.0	-4.1	-1.1	-2.3	-1.5	0.1	-0.5	-2.6	-3.3	-9.6	-6.3	-12.1	-7.5	-1.8	-15.1
2370	1.3	-1.5	0.1	0.4	-0.3	-0.2	0.1	0.7	2.5	0.2	-3.2	-0.6	-2.1	-0.3	0.6	-0.1
2450	-0.4	-1.5	1.6	0.2	-0.7	-0.2	0.3	-0.2	4.4	2.8	-3.0	-0.7	-2.6	1.2	-0.2	4.4
2470	-24.8	-16.3	-16.1	-2.1	-4.3	-5.0	0.6	1.6	0.6	-4.4	-17.4	-16.1	-57.8	-24.0	-2.6	-28.1
2600	-1.3	-3.9	-4.9	-1.7	-3.3	-0.4	1.0	0.8	4.7	-3.9	-10.0	-1.1	-7.6	-9.3	1.7	-10.6
2730	-8.6	-5.3	-3.5	-1.6	-3.2	-1.3	1.5	1.4	2.5	-5.0	-3.7	-7.4	-21.4	-7.9	1.7	-4.2
2740	-3.2	0.4	0.0	2.3	-0.1	-1.9	0.7	1.1	4.8	-0.3	1.1	0.7	-1.9	2.2	-0.2	6.8
2960	-8.6	-2.7	-1.2	-2.4	-6.4	-3.9	0.4	1.5	-3.2	-3.4	-9.6	-10.7	-25.2	-10.3	-3.1	-16.2
3050	-10.3	-5.9	0.4	0.0	-3.5	-5.8	1.3	2.3	-0.7	-1.9	-2.6	-6.4	-22.9	-1.9	-2.6	-5.4
3100	-2.5	1.6	5.1	1.8	-1.8	1.4	1.4	2.0	5.1	1.5	2.3	-0.8	-7.1	4.5	4.9	8.7

Table 6 | Results of the trend analysis ($^{\circ}\text{C}/10$ years) for the monthly and seasonal mean temperature (significant values are marked in bold)

ID	January	February	March	April	May	June	July	August	September	October	November	December	Winter	Spring	Summer	Autumn
930	0.01	-0.11	0.01	-0.09	0.06	0.07	0.02	0.06	-0.13	-0.07	-0.12	-0.06	-0.06	-0.03	0.06	-0.10
1010	0.00	-0.12	-0.03	-0.13	0.04	-0.08	-0.14	-0.04	-0.23	-0.10	-0.17	-0.08	-0.08	-0.05	-0.10	-0.19
1100	-0.07	-0.32	-0.03	0.00	0.08	0.06	0.11	0.03	-0.14	0.11	-0.14	-0.18	-0.23	0.00	0.09	-0.10
1130	0.04	-0.08	-0.03	0.02	0.09	0.20	0.24	0.21	-0.02	0.03	-0.14	-0.09	-0.07	0.00	0.22	-0.07
1180	-0.02	-0.01	-0.02	-0.02	0.14	-0.02	-0.12	-0.04	-0.18	-0.10	-0.16	0.20	0.06	0.04	-0.06	-0.15
1330	0.05	-0.02	0.04	-0.02	-0.13	-0.10	-0.28	-0.06	0.08	0.00	0.03	-0.11	-0.09	-0.09	-0.16	0.05
1460	-0.09	-0.36	-0.39	-0.30	-0.26	-0.17	-0.30	-0.09	0.04	0.02	-0.04	-0.12	-0.16	-0.32	-0.19	0.01
1550	0.05	0.05	0.08	0.07	0.01	0.02	-0.04	0.09	0.18	0.24	0.12	0.00	0.08	-0.01	0.01	0.17
1680	0.19	0.13	0.07	-0.03	0.12	0.17	0.09	0.10	-0.06	0.01	0.00	0.15	0.17	0.04	0.12	-0.02
1760	0.03	-0.02	0.06	0.08	0.16	0.13	0.08	0.12	-0.05	0.03	-0.07	0.13	0.07	0.09	0.13	-0.03
1850	0.13	0.08	0.10	0.06	0.17	0.10	0.10	0.14	-0.04	0.07	-0.02	0.04	0.07	0.10	0.12	0.01
1960	0.07	-0.04	-0.02	-0.11	0.07	0.00	-0.02	-0.02	-0.18	-0.08	-0.12	0.00	-0.02	-0.03	0.00	-0.12
1970	0.08	0.04	0.13	0.09	0.27	0.42	0.32	0.27	-0.02	0.07	-0.12	0.00	0.03	0.13	0.34	-0.04
1980	0.08	0.00	0.03	-0.03	0.12	0.02	0.00	0.09	-0.04	0.01	-0.08	0.02	0.04	0.06	0.03	-0.04
2120	-0.02	-0.07	-0.04	-0.09	0.12	0.08	0.01	-0.01	-0.12	-0.01	-0.16	-0.11	-0.06	0.01	0.03	-0.08
2170	-0.11	-0.23	-0.11	-0.22	0.00	0.02	0.02	0.03	-0.17	-0.12	-0.22	-0.21	-0.17	-0.10	0.01	-0.17
2180	-0.09	-0.33	-0.14	-0.12	-0.16	-0.14	-0.04	-0.06	-0.36	-0.18	-0.32	-0.23	-0.27	-0.14	-0.11	-0.30
2210	0.00	-0.15	-0.05	-0.27	0.00	-0.13	-0.19	-0.16	-0.33	-0.09	-0.13	-0.08	-0.07	-0.11	-0.16	-0.21
2330	0.30	0.40	0.30	0.24	-0.02	0.07	0.19	0.12	-1.37	-0.25	-0.06	-0.06	-0.66	0.17	0.13	-0.86
2370	-0.05	-0.16	0.04	-0.02	0.15	0.23	0.16	0.22	-0.01	0.01	-0.15	-0.13	-0.12	0.09	0.19	-0.07
2450	0.18	0.09	0.08	0.10	0.17	0.18	0.22	0.21	0.01	0.05	-0.04	0.07	0.11	0.12	0.20	0.00
2470	-0.05	-0.12	-0.08	-0.06	-0.02	0.06	-0.02	-0.06	-0.35	-0.13	-0.13	-0.10	-0.12	-0.05	-0.01	-0.21
2600	0.11	-0.10	0.16	0.12	0.28	0.14	0.23	0.20	-0.11	0.05	-0.02	-0.08	-0.02	0.18	0.17	-0.03
2730	0.05	-0.05	-0.08	-0.18	0.04	-0.08	-0.13	-0.01	-0.16	-0.07	-0.15	0.00	-0.03	-0.05	-0.08	-0.15
2740	0.05	-0.08	-0.01	-0.02	0.01	-0.01	-0.01	-0.08	-0.18	-0.14	-0.10	-0.02	-0.03	-0.01	-0.05	-0.11
2960	-0.13	-0.19	-0.14	-0.17	0.11	0.08	0.12	0.17	-0.01	-0.01	-0.16	-0.06	-0.16	-0.07	0.09	-0.06
3050	-0.03	-0.19	-0.25	-0.30	-0.08	-0.14	-0.25	-0.21	-0.24	-0.11	-0.21	-0.07	-0.14	-0.18	-0.23	-0.19
3100	0.16	-0.08	0.01	0.04	0.05	-0.01	-0.05	-0.20	-0.31	-0.14	-0.04	-0.01	0.04	0.04	-0.07	-0.16

Table 7 | Results of the trend analysis ($^{\circ}\text{C}/10$ years) for the monthly and seasonal maximum temperature (significant values are marked in bold)

ID	January	February	March	April	May	June	July	August	September	October	November	December	Winter	Spring	Summer	Autumn
930	0.08	-0.09	0.00	-0.11	0.03	0.03	-0.03	0.00	-0.21	-0.10	-0.11	-0.08	-0.04	-0.05	0.01	-0.14
1010	0.07	-0.03	0.07	-0.11	0.08	-0.11	-0.19	-0.09	-0.30	-0.01	-0.08	-0.01	-0.02	-0.01	-0.15	-0.16
1100	-0.04	-0.23	0.02	0.11	0.25	0.19	0.15	0.20	-0.19	0.16	-0.01	-0.16	-0.13	0.11	0.16	-0.07
1130	0.05	0.06	0.06	0.12	0.23	0.27	0.20	0.16	-0.14	0.11	-0.17	-0.19	-0.04	0.10	0.21	-0.08
1180	-0.02	0.02	-0.12	-0.21	0.04	-0.05	-0.17	-0.16	-0.30	-0.12	-0.18	0.09	0.03	-0.07	-0.12	-0.20
1330	-0.04	-0.11	-0.11	-0.37	-0.16	-0.30	-0.08	-0.32	-0.51	-0.40	-0.48	-0.23	-0.12	-0.22	-0.34	-0.48
1460	-0.10	-0.14	-0.21	-0.37	-0.45	-0.78	-0.84	-0.69	-0.55	-0.36	-0.44	-0.22	-0.16	-0.35	-0.73	-0.44
1550	0.25	0.25	0.09	-0.25	0.08	0.00	0.09	0.09	0.14	0.34	0.22	0.41	0.23	-0.05	0.02	0.21
1680	0.04	-0.01	-0.10	-0.31	-0.18	-0.15	-0.20	-0.24	-0.39	-0.26	-0.18	0.02	0.01	-0.23	-0.20	-0.27
1760	-0.02	-0.06	0.06	0.09	0.15	0.04	0.00	0.06	-0.06	0.02	-0.11	0.11	0.05	0.11	0.06	-0.03
1850	0.05	-0.01	0.02	-0.03	0.10	0.01	0.01	0.02	-0.18	-0.04	-0.11	-0.02	0.00	0.02	0.02	-0.11
1960	0.12	0.01	0.04	-0.11	0.08	-0.10	-0.12	-0.13	-0.26	-0.02	-0.02	0.06	0.04	0.00	-0.10	-0.10
1970	0.16	0.22	0.30	0.19	0.33	0.51	0.32	0.26	0.00	0.12	-0.01	0.14	0.17	0.24	0.37	0.02
1980	0.07	0.03	0.08	-0.02	0.17	-0.02	0.00	0.03	-0.18	0.07	-0.02	0.00	0.02	0.08	0.00	-0.05
2120	-0.24	-0.23	-0.19	-0.28	-0.02	-0.08	-0.13	-0.25	-0.31	-0.21	-0.31	-0.25	-0.25	-0.13	-0.14	-0.26
2170	-0.13	-0.24	-0.07	-0.19	0.04	0.06	0.03	0.04	-0.19	-0.11	-0.22	-0.24	-0.18	-0.06	0.04	-0.17
2180	-0.04	-0.27	-0.04	-0.11	-0.12	-0.13	-0.07	-0.04	-0.38	-0.16	-0.34	-0.19	-0.25	-0.08	-0.10	-0.32
2210	0.05	-0.04	0.01	-0.19	0.03	-0.09	-0.19	-0.16	-0.36	-0.05	-0.12	-0.03	0.00	-0.06	-0.15	-0.20
2330	-2.13	-0.42	-0.16	-0.29	0.11	0.17	0.07	-0.02	-0.24	-0.12	0.10	0.04	-2.30	-0.11	0.07	-0.09
2370	-0.14	-0.22	0.03	-0.04	0.07	0.25	0.22	0.22	-0.02	0.01	-0.17	-0.19	-0.19	0.05	0.21	-0.09
2450	0.06	0.04	0.00	0.01	0.07	0.07	0.12	0.06	-0.14	-0.09	-0.17	-0.06	0.02	0.03	0.07	-0.14
2470	-0.10	-0.14	-0.15	-0.13	-0.15	-0.02	-0.10	-0.23	-0.51	-0.26	-0.21	-0.20	-0.16	-0.14	-0.13	-0.33
2600	0.07	0.03	0.09	0.06	0.25	0.15	0.15	0.10	-0.12	0.05	-0.04	0.00	0.03	0.13	0.14	-0.04
2730	-0.19	-0.28	-0.29	-0.48	-0.25	-0.46	-0.49	-0.39	-0.57	-0.40	-0.44	-0.25	-0.26	-0.33	-0.44	-0.51
2740	0.08	-0.02	0.04	-0.05	-0.07	-0.09	0.02	-0.14	-0.25	-0.06	0.02	0.04	0.00	-0.05	-0.04	-0.08
2960	-0.04	-0.09	-0.11	-0.14	0.14	0.10	0.13	0.15	-0.01	-0.05	-0.16	-0.11	-0.10	-0.04	0.11	-0.07
3050	-0.10	-0.28	-0.37	-0.43	-0.19	-0.33	-0.46	-0.45	-0.44	-0.23	-0.27	-0.16	-0.23	-0.30	-0.46	-0.31
3100	0.06	-0.14	-0.16	-0.18	-0.08	-0.24	-0.30	-0.34	-0.46	-0.23	-0.01	-0.02	-0.02	-0.13	-0.27	-0.23

Table 8 | Results of the trend analysis ($^{\circ}\text{C}/10$ years) for the monthly and seasonal minimum temperature (significant values are marked in bold)

ID	January	February	March	April	May	June	July	August	September	October	November	December	Winter	Spring	Summer	Autumn
930	-0.05	-0.13	0.03	-0.07	0.09	0.11	0.06	0.13	-0.04	-0.05	-0.13	-0.03	-0.09	-0.01	0.11	-0.06
1010	-0.08	-0.20	-0.12	-0.15	0.00	-0.06	-0.09	0.01	-0.15	-0.18	-0.26	-0.16	-0.13	-0.09	-0.05	-0.22
1100	-0.10	-0.39	-0.09	-0.11	-0.10	-0.06	0.08	-0.11	-0.04	0.07	-0.27	-0.19	-0.27	-0.11	0.03	-0.12
1130	-0.01	-0.27	-0.16	-0.11	-0.06	0.09	0.29	0.27	0.12	-0.01	-0.14	0.00	-0.12	-0.13	0.22	-0.04
1180	-0.01	-0.03	0.08	0.17	0.24	0.00	-0.09	0.07	-0.07	-0.07	-0.14	0.31	0.09	0.15	0.01	-0.10
1330	0.26	0.27	0.30	0.27	0.26	0.20	-0.07	0.11	0.20	0.12	0.17	0.14	0.15	0.21	0.09	0.18
1460	0.28	0.07	0.07	0.10	0.02	0.02	-0.15	0.04	0.19	0.17	0.14	0.12	0.21	0.01	-0.04	0.16
1550	0.05	0.05	0.08	0.07	0.01	0.02	-0.04	0.09	0.18	0.24	0.12	0.00	0.08	-0.01	0.01	0.17
1680	0.35	0.28	0.29	0.24	0.40	0.49	0.37	0.44	0.26	0.28	0.17	0.29	0.32	0.31	0.44	0.24
1760	0.09	0.03	0.06	0.07	0.17	0.22	0.16	0.18	-0.03	0.05	-0.03	0.14	0.09	0.08	0.19	-0.03
1850	0.22	0.16	0.18	0.14	0.24	0.19	0.19	0.26	0.11	0.18	0.07	0.10	0.15	0.18	0.21	0.13
1960	0.01	-0.09	-0.08	-0.12	0.06	0.09	0.09	0.08	-0.10	-0.14	-0.22	-0.07	-0.07	-0.05	0.09	-0.15
1970	0.01	-0.13	-0.04	-0.02	0.21	0.34	0.32	0.29	-0.03	0.02	-0.22	-0.14	-0.12	0.02	0.30	-0.10
1980	0.08	-0.03	-0.02	-0.04	0.08	0.05	0.00	0.15	0.10	-0.05	-0.14	0.05	0.05	0.03	0.07	-0.04
2120	0.19	0.09	0.11	0.10	0.26	0.24	0.14	0.23	0.06	0.19	-0.01	0.03	0.13	0.15	0.19	0.10
2170	-0.09	-0.22	-0.14	-0.25	-0.04	-0.02	0.02	0.02	-0.15	-0.13	-0.21	-0.17	-0.16	-0.14	-0.01	-0.16
2180	-0.14	-0.40	-0.23	-0.12	-0.20	-0.15	0.00	-0.08	-0.34	-0.20	-0.29	-0.28	-0.30	-0.20	-0.11	-0.29
2210	-0.06	-0.26	-0.12	-0.34	-0.04	-0.16	-0.19	-0.17	-0.31	-0.14	-0.14	-0.13	-0.13	-0.15	-0.17	-0.21
2330	0.49	0.64	0.54	0.49	0.19	0.27	0.29	0.19	-0.60	-0.08	0.03	0.16	0.77	0.41	0.25	-0.32
2370	0.03	-0.10	0.05	0.00	0.22	0.21	0.09	0.22	0.00	0.00	-0.14	-0.07	-0.05	0.13	0.16	-0.06
2450	0.30	0.14	0.15	0.18	0.28	0.30	0.31	0.35	0.16	0.20	0.10	0.20	0.20	0.21	0.33	0.15
2470	-0.02	-0.14	-0.03	0.00	0.10	0.12	0.06	0.12	-0.19	0.06	-0.03	-0.07	-0.11	0.03	0.09	-0.06
2600	0.01	-0.23	0.02	-0.02	0.16	0.03	0.13	0.14	-0.09	-0.05	-0.10	-0.12	-0.14	0.04	0.09	-0.08
2730	0.28	0.18	0.13	0.12	0.33	0.30	0.22	0.38	0.24	0.26	0.13	0.24	0.21	0.22	0.28	0.20
2740	0.04	-0.08	0.02	0.06	0.11	0.08	0.05	0.01	-0.06	-0.16	-0.20	-0.04	-0.04	0.08	0.02	-0.09
2960	-0.16	-0.29	-0.17	-0.18	0.07	0.07	0.13	0.21	0.00	-0.04	-0.18	-0.01	-0.18	-0.10	0.11	-0.09
3050	-0.03	-0.11	-0.13	-0.16	0.02	0.04	-0.04	0.04	-0.03	0.00	-0.15	0.01	-0.05	-0.06	-0.01	-0.08
3100	0.28	-0.07	0.16	0.26	0.19	0.25	0.22	-0.07	-0.19	-0.07	-0.04	-0.02	0.09	0.21	0.16	-0.09

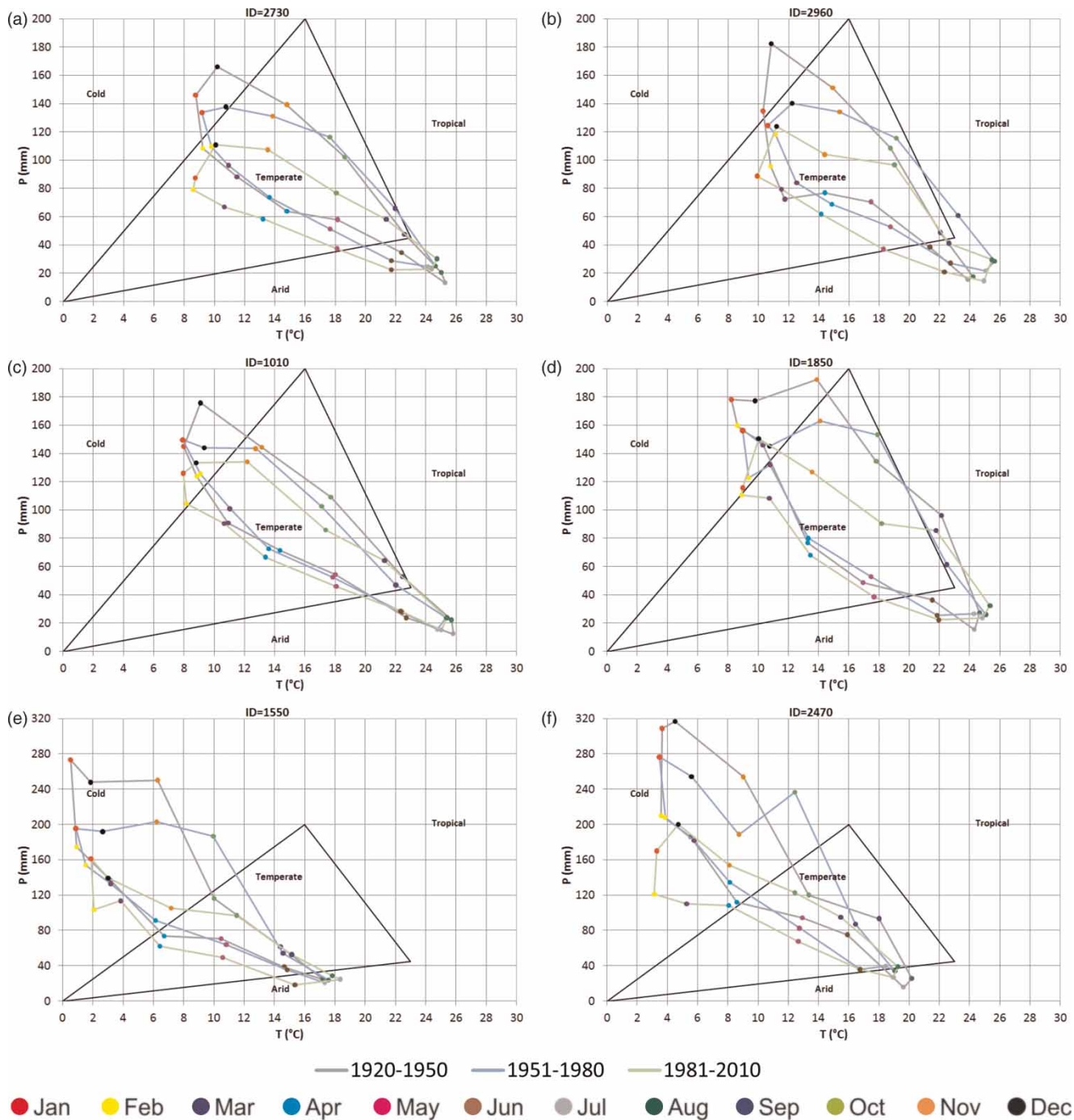


Figure 6 | Examples of the variation of the Péguy climographs with reference to three sub-periods: (a), (b) gauges with elevation lower than 80 m a.s.l.; (c), (d) gauges with elevation from 80 to 400 m a.s.l.; (e), (f) gauges with elevation higher than 400 m a.s.l.

The combined analysis of precipitation and temperature data has proved to be very useful for the identification of the main climatic features of a region. In particular, this kind of approach, based on the homogeneity analysis of

temperature/rainfall data and on geostatistical interpolation techniques, can be realistically assumed for the spatial characterization of the climatic variables in areas like Calabria, which are particularly complex from an orographic and

a hydrological point of view. Moreover, the application of the Peguy climograph is an easy way to characterize the climate of a region, because it requires only homogeneous rainfall and temperature data at monthly scale, available on a long time span (at least 60 years). Actually, its application is repeatable in other geographical areas, also characterized by different climatic features.

ACKNOWLEDGEMENTS

The research was supported by 'AQUA – Gestione sostenibile della risorsa acqua in agricoltura. Task 1.1 – Variabilità meteo-climatica ed eventi estremi di precipitazione e siccità nell'Europa Mediterranea. Decreto MIUR n. 973/2013. Department of Bio-Agrifood Science, National Research Council of Italy.

The authors thank the reviewers of this paper for providing constructive comments, which have contributed to the improvement of the published version.

REFERENCES

- Alexandersson, H. 1986 A homogeneity test applied to precipitation data. *Int. J. Climatol.* **6**, 661–675.
- Aznar, J. C., Gloaguen, E., Tapsoba, D., Hachem, S., Caya, D. & Bégin, Y. 2013 Interpolation of monthly mean temperatures using cokriging in spherical coordinates. *Int. J. Climatol.* **33**, 758–769.
- Bajat, B., Pejović, M., Luković, J., Manojlović, P., Ducić, V. & Mustafić, S. 2013 Mapping average annual precipitation in Serbia (1961–1990) by using regression kriging. *Theor. Appl. Climatol.* **112**, 1–13.
- Brunetti, M., Buffoni, L., Mangianti, F., Maugeri, M. & Nanni, T. 2004 Temperature, precipitation and extreme events during the last century in Italy. *Global Planet. Change* **40**, 141–149.
- Brunetti, M., Maugeri, M., Monti, F. & Nanni, T. 2006a Temperature and precipitation variability in Italy in the last two centuries from homogenised instrumental time series. *Int. J. Climatol.* **26**, 345–381.
- Brunetti, M., Nanni, T., Maugeri, M., Auer, I., Boehm, R. & Schoener, W. 2006b Precipitation variability and changes in the Greater Alpine Region over the 1800–2003 period. *J. Geophys. Res. Atmos.* **111**, D11, D11107.
- Brunetti, M., Caloiero, T., Coscarelli, R., Gullà, G., Nanni, T. & Simolo, C. 2012 Precipitation variability and change in the Calabria region (Italy) from a high resolution daily dataset. *Int. J. Climatol.* **32**, 57–73.
- Buttafuoco, G., Caloiero, T. & Coscarelli, R. 2011 Spatial and temporal patterns of the mean annual precipitation at decadal time scale in southern Italy (Calabria region). *Theor. Appl. Climatol.* **105**, 431–444.
- Caloiero, T., Coscarelli, R., Ferrari, E. & Mancini, M. 2011a Trend detection of annual and seasonal rainfall in Calabria (Southern Italy). *Int. J. Climatol.* **31**, 44–56.
- Caloiero, T., Coscarelli, R., Ferrari, E. & Mancini, M. 2011b Precipitation change in Southern Italy linked to global scale oscillation indexes. *Nat. Hazards Earth Syst. Sci.* **11**, 1–12.
- Capra, A., Consoli, S. & Scicolone, B. 2013 Long-term climatic variability in Calabria and effects on drought and agrometeorological parameters. *Water Resour. Manage.* **27**, 601–617.
- Chilès, J. P. & Delfiner, P. 2012 *Geostatistics: Modelling Spatial Uncertainty*, 2nd edn. Wiley, New York.
- Coscarelli, R. & Caloiero, T. 2012 Analysis of daily and monthly rainfall concentration in Southern Italy (Calabria region). *J. Hydrol.* **416–417**, 145–156.
- Craddock, J. M. 1979 Methods of comparing annual rainfall records for climatic purposes. *Weather* **34**, 332–346.
- del Rio, S., Herrero, L., Fraile, R. & Penas, A. P. 2011 Spatial distribution of recent rainfall trends in Spain (1961–2006). *Int. J. Climatol.* **31**, 656–667.
- del Rio, S., Cano-Ortiz, A., Herrero, L. & Penas, A. P. 2012 Recent trends in mean maximum and minimum air temperatures over Spain (1961–2006). *Theor. Appl. Climatol.* **109**, 605–626.
- Diodato, N. & Ceccarelli, M. 2005 Interpolation processes using multivariate geostatistics for mapping of climatological precipitation mean in the Sannio Mountains (southern Italy). *Earth Surf. Proc. Land.* **30**, 259–268.
- Diodato, N., Bellocchi, G., Bertolin, C. & Camuffo, D. 2013 Mixed nonlinear regression for modelling historical temperatures in Central-Southern Italy. *Theor. Appl. Climatol.* **113**, 187–196.
- Donat, M. G. & Alexander, L. V. 2012 The shifting probability distribution of global daytime and night-time temperatures. *Geophys. Res. Lett.* **39**, L14707.
- Easterling, D. R., Horton, B., Jones, P. D., Peterson, T. C., Karl, T. R., Parker, D. E., Salinger, M. J., Razuvayev, V., Plummer, N., Jamason, P. & Folland, C. K. 1997 Maximum and minimum temperature trends for the globe. *Science* **277**, 364–367.
- Faticchi, S. & Caporali, E. 2009 A comprehensive analysis of changes in precipitation regime in Tuscany. *Int. J. Climatol.* **29**, 1883–1893.
- Feidas, H., Nouloupoulou, Ch., Makrogiannis, T. & Bora-Senta, E. 2007 Trend analysis of precipitation time series in Greece and their relationship with circulation using surface and satellite data: 1955–2001. *Theor. Appl. Climatol.* **87**, 155–177.
- Ferrari, E., Caloiero, T. & Coscarelli, R. 2013 Influence of the North Atlantic Oscillation on winter rainfall in Calabria (southern Italy). *Theor. Appl. Climatol.* **14**, 479–494.
- Goovaerts, P. 1997 *Geostatistics for Natural Resources Evaluation*. Oxford University Press, New York.

- Grimes, I. F. & Pardo-Iguzquiza, E. 2010 Geostatistical analysis of rainfall. *Geogr. Anal.* **42**, 136–160.
- Helldén, U. & Tottrup, C. 2008 Regional desertification: a global synthesis. *Global Planet. Change* **64**, 169–176.
- Hudson, G. & Wackernagel, H. 1994 Mapping temperature using kriging with external drift: theory and an example from Scotland. *Int. J. Climatol.* **14**, 77–91.
- Incerti, G., Feoli, E., Giovacchini, A., Salvati, L. & Brunetti, A. 2007 Analysis of bioclimatic time series and their neural network-based classification to characterize drought risk patterns in south Italy. *Int. J. Biometeorol.* **51**, 253–263.
- IPCC 2013 Summary for Policymakers. Fifth Assessment Report of the Intergovernmental Panel on Climate Change. Cambridge University Press, Cambridge.
- Jones, P. D. 1995 The instrumental data record: its accuracy and use in attempts to identify the ‘CO₂’ signal. In: *Analysis of Climate Variability* (H. von Storch & A. Navarra, eds). Springer-Verlag, Berlin, pp. 53–76.
- Karl, T. R. & Williams, C. N. 1987 An approach to adjusting climatological time series for discontinuous inhomogeneity. *J. Clim. Appl. Meteorol.* **26**, 1744–1763.
- Kendall, M. G. 1962 *Rank Correlation Methods*. Hafner Publishing Company, New York.
- Klein Tank, A. M. G. & Können, G. P. 2003 Trends in indices of daily temperature and precipitation extremes in Europe 1946–99. *J. Climate* **16**, 3665–3680.
- Klok, E. J. & Tank, A. 2009 Updated and extended European dataset of daily climate observations. *Int. J. Climatol.* **29**, 1182–1191.
- Mann, H. B. 1945 Nonparametric tests against trend. *Econometrica* **13**, 245–259.
- Matheron, G. 1971 *The Theory of Regionalised Variables and its Applications*. Les Cahiers du Centre de Morphologie Mathématique de Fontainebleau n.5, Paris, France.
- Palmieri, S., Siani, A. M. & D’Agostino, A. 1991 Climate fluctuations and trends in Italy within the last hundred years. *Ann. Geophys.* **9**, 769–776.
- Pavan, V., Tomozeiu, R., Cacciamani, C. & Di Lorenzo, M. 2008 Daily precipitation observations over Emilia-Romagna: mean values and extremes. *Int. J. Climatol.* **28**, 2065–2079.
- Péguy, C. P. 1961 Une tentative de délimitation et de schématisation des climats intertropicaux. *Rev. Geogr. Lyon* **36**, 1–6.
- Peterson, T. C. & Easterling, D. R. 1994 Creating of homogeneous composite climatological reference series. *Int. J. Climatol.* **14**, 671–679.
- Rivoirard, J. 1994 *Introduction to Disjunctive Kriging and Non-linear Geostatistics*. Oxford University Press, Oxford.
- Sánchez, E., Gallardo, C., Gaertner, M. A., Arribas, A. & Castro, M. 2004 Future climate extreme events in the Mediterranean simulated by a regional climate model: a first approach. *Glob. Planet. Change* **44**, 163–180.
- Toreti, A. & Desiato, F. 2008 Temperature trend over Italy from 1961 to 2004. *Theor. Appl. Climatol.* **91**, 51–58.
- Toreti, A., Desiato, F., Fioravanti, G. & Perconti, W. 2009 Annual and seasonal precipitation over Italy from 1961 to 2006. *Int. J. Climatol.* **29**, 1976–1987.
- Ventura, F., Rossi Pisa, P. & Ardizzoni, E. 2002 Temperature and precipitation trends in Bologna (Italy) from 1952 to 1999. *Atmos. Res.* **61**, 203–214.
- Vergni, L. & Todisco, F. 2011 Spatio-temporal variability of precipitation, temperature and agricultural drought indices in Central Italy. *Agr. Forest Meteorol.* **151**, 301–313.
- Von Hardenberg, J., Ciccarelli, N., Provenzale, A., Ronchi, C., Vargiu, A. & Pelosini, R. 2008 Variabilità climatica in Italia nord-occidentale nella seconda metà del XX secolo. In: *Clima e Cambiamenti Climatici – Le attività di Ricerca del CNR* (B. Carli, G. Cavarretta, M. Colacino & S. Fuzzi, eds). Consiglio Nazionale delle Ricerche, Roma, pp. 221–224.
- Vose, R. S., Easterling, D. R. & Gleason, B. 2005 Maximum and minimum temperature trends for the globe: an update through, 2004. *Geophys. Res. Lett.* **32**, L23824.
- Wackernagel, H. 2003 *Multivariate Geostatistics: an Introduction with Applications*. Springer-Verlag, Berlin.
- Webster, R. & Oliver, M. A. 2007 *Geostatistics for Environmental Scientists*. Wiley, Chichester.
- Xoplaki, E., Luterbacher, J. & González-Rouco, J. F. 2006 Mediterranean summer temperature and winter precipitation, large-scale dynamics, trends. *Nuovo Cimento* **29**, 45–54.
- Zhou, X. & Wang, Y. 2011 Dynamics of land surface temperature in response to land-use/cover change. *Geogr. Res.* **49**, 23–36.

First received 30 January 2014; accepted in revised form 27 June 2014. Available online 17 July 2014